

Coulomb Correlations and Orbital Polarization in the Metal Insulator Transition of VO₂

A. Liebsch¹, H. Ishida², and G. Bihlmayer¹

¹*Institut für Festkörperforschung, Forschungszentrum Jülich, 52425 Jülich, Germany*

²*College of Humanities and Sciences, Nihon University, Sakura-josui, Tokyo 156, Japan*

The quasi-particle spectra in the metallic rutile and insulating monoclinic phases of VO₂ are shown to be dominated by local Coulomb interactions. In the rutile phase the small orbital polarization among V 3d t_{2g} states leads to weak static but strong dynamical correlations. In the monoclinic phase the large 3d orbital polarization caused by the V–V Peierls distortion gives rise to strong static correlations which are shown to be the primary cause of the insulating behavior.

PACS numbers: 71.20.Be, 71.27.+a, 79.60.Bm

I. INTRODUCTION

The metal insulator transition in VO₂ has been intensively studied for a long time. At 340 K the resistivity changes by several orders of magnitude.¹ The high-temperature metallic phase has a rutile structure, while the low-temperature insulating phase is monoclinic (M_1), with a zigzag-type pairing of V atoms along the c axis. Both phases are non-magnetic. Although this transition is widely regarded as a Mott-Hubbard transition,^{2,3,4,5} the role of the Peierls distortion of the crystal structure in the insulating phase has been the topic of intense debate.^{6,7,8,9,10,11,12,13} The discovery of a second insulating phase (M_2),² in which only half of the V atoms form pairs while the other evenly spaced chains behave as magnetic insulators, suggested that both low temperature phases should be regarded as Mott-Hubbard and not as Peierls band insulators.^{3,5} Although the role of the Coulomb interaction in the metal insulator transition of VO₂ has been studied previously,^{10,11,12,13} a consistent description of the rutile and monoclinic phases is not yet available.

The aim of the present work is to elucidate the interplay of Coulomb correlations and orbital polarization in the quasi-particle spectra of VO₂. Analyzing recent photoemission data^{14,15} we demonstrate that the metallic and insulating phases show evidence of strong local interactions which manifest themselves in distinctly different ways because of the different degree of orbital polarization in the rutile and monoclinic structures. The key aspect of the metallic phase is the small orbital polarization among V 3d t_{2g} states, implying weak static but strong dynamical correlations. Thus, the spectra reveal band narrowing and reduced weight of the coherent peak near the Fermi level, and an incoherent satellite feature associated with the lower Hubbard band. The monoclinic phase, in contrast, is characterized by a pronounced t_{2g} orbital polarization induced by the V–V Peierls distortion. The local Coulomb interaction therefore leads to strong static correlations and to the opening of an excitation gap. The influence of non-diagonal coupling among t_{2g} orbitals on the size of the gap is investigated within

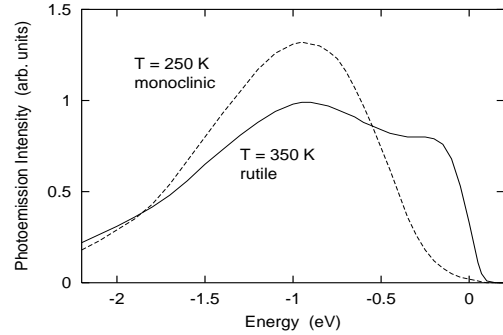


FIG. 1: Measured photoemission spectra for VO₂ films on TiO₂ in the V 3d band region after background subtraction. Solid curve: $T = 350$ K (metallic rutile phase); dashed curve: $T = 250$ K (insulating monoclinic phase); $E_F = 0$.¹⁴

the static limit and is found to be small.

In the following sections we discuss results obtained within several theoretical approaches, such as the dynamical mean field theory (DMFT)¹⁶, the local density approximation plus Hubbard U (LDA+ U)¹⁷ and GW ¹⁸ methods. We argue that none is presently capable of explaining all of the observed phenomena in a consistent manner. Instead, we focus on the merits and failures of these approaches with the aim of highlighting the different roles of Coulomb correlations and orbital polarization in the metallic and insulating phases of VO₂.

II. RESULTS AND DISCUSSION

Fig. 1 shows photoemission spectra for VO₂ films (150 Å thick) grown on TiO₂(001) at binding energies corresponding to the V 3d bands (21.2 eV photon energy).¹⁴ Emission from O 2p states extends from -2 eV to about -8 eV. As a result of compressive stress from the substrate¹⁹ the transition temperature is lowered from 340 K to 290 K. The high temperature spectrum shows a Fermi edge characteristic of metallic behavior which is absent in the low temperature spectrum. While this trend is in agreement with previous photoemission

measurements,^{20,21} the data in Fig. 1 reveal two spectral features in the metallic phase: a peak close to E_F and a second one near -1 eV. In the insulating phase, the peak near E_F disappears and the feature near -1 eV becomes more intense. Recent VO_2 photoemission spectra taken at 520 eV photon energy¹⁵ agree with the ones shown in Fig. 1, except for a considerably greater relative weight of the coherent peak near E_F in the metallic phase. These spectral changes are consistent with the observation that satellite peaks in low photon energy spectra tend to be more pronounced as a result of a surface induced enhancement of Coulomb correlations.^{22,23,24}

Before analyzing the photoemission data we discuss the single particle properties of VO_2 obtained using density functional theory. We have carried out full potential linearized augmented plane wave (LAPW) calculations for the rutile and monoclinic structures using the experimental lattice parameters and treating exchange correlation within the generalized gradient approximation (GGA).²⁵ Due to the octahedral crystal field, the states near E_F have V $3d$ t_{2g} character. They are separated by a small gap from the empty e_g states, and from the O $2p$ states by a gap of about 1.0 eV. The occupancy of the t_{2g} manifold is $3d^1$. Our results qualitatively confirm previous LDA calculations.^{8,9,10,11} Fig. 2(a) shows a comparison of the V total t_{2g} density of states for the rutile and monoclinic phases of VO_2 . Although there are differences in detail, the overall width of these distributions and the shape of the occupied region are similar for both structures. Evidently, the GGA/LDA does not predict the insulating nature of the monoclinic phase. Moreover, on the basis of these densities one would not expect correlations to play very different roles in the two phases. However, if we plot the subband contributions to the t_{2g} density, the two structures are very different, as shown in Figs. 2(b) and (c). Whereas in the rutile phase the t_{2g} bands have similar occupation numbers, in the monoclinic phase the $d_{x^2-y^2}$ band is significantly more occupied than the $d_{xz,yz}$ bands. (We adopt the local coordinate system of Ref. 6, i.e., x denotes the c axis, while y and z point along the diagonals of the a, b plane.) The origin of this orbital polarization is the V-V dimerization along the c axis. The $d_{x^2-y^2}$ band splits into bonding and anti-bonding components, while the $d_{xz,yz}$ bands are pushed upwards due to shortening of V-O distances. Investigation of the energy bands shows that, in agreement with earlier work,^{8,9} the top of the bonding $d_{x^2-y^2}$ bands is separated by a slight negative gap from the bottom of the $d_{xz,yz}$ bands. In the following subsection we show that different degree of orbital polarization in the rutile and monoclinic phases has a pronounced effect on the quasi-particle spectra of VO_2 .

A. Metallic Rutile Phase

Let us first discuss the rutile phase. Comparing the t_{2g} density of states with the photoemission spectra it is

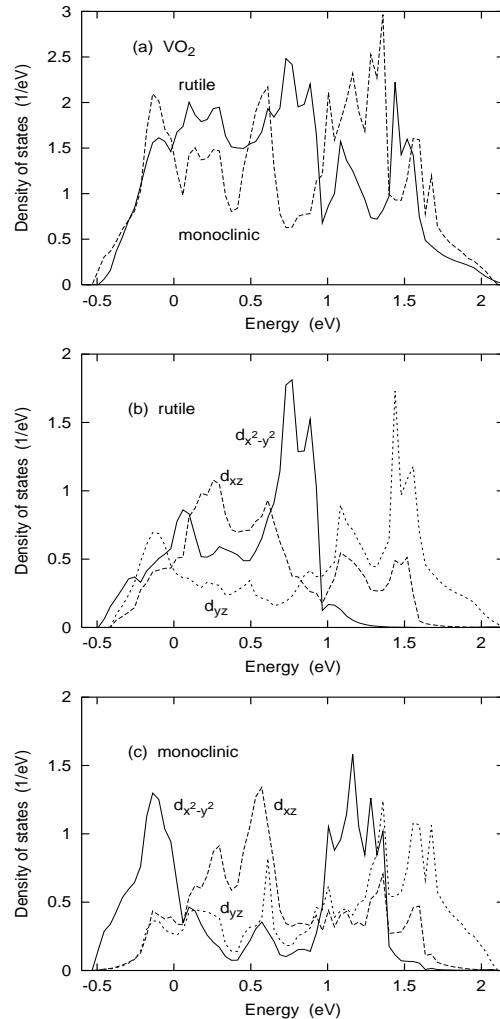


FIG. 2: VO_2 $3d$ density of states calculated within LAPW method. (a) Total t_{2g} densities for rutile and monoclinic phases; (b) and (c) t_{2g} density of states components for rutile and monoclinic phases; $E_F = 0$.

plausible to associate the feature close to E_F with emission from metallic V $3d$ states. The peak near -1 eV, however, lies in the gap between V $3d$ and O $2p$ states and cannot be understood within the single particle picture. To describe the spectra in the rutile phase it is clearly necessary to account for dynamical Coulomb correlations. For the evaluation of the quasi-particle distributions we use the Dynamical Mean Field Theory combined with the multiband Quantum Monte Carlo (QMC) method.¹⁶ Since hybridization among t_{2g} states is weak the local self-energy is taken as diagonal in orbital space. The t_{2g} density of states components shown in Fig. 2(b) then serve as input quantities accounting for the single particle properties of the rutile structure. The local Coulomb interaction defining the quantum impurity problem is characterized by intra- and inter-orbital matrix elements U and $U' = U - 2J$, where J is the Hund's rule exchange integral. According to constrained LDA

calculations, $U \approx 4.2\text{eV}$ and $J \approx 0.8\text{eV}$.^{11,26} The calculations are performed at $T \approx 500\text{K}$ with up to 10^6 sweeps. The quasi-particle distributions are obtained via maximum entropy reconstruction.²⁷

Fig. 3(a) shows that, in contrast to the single particle density of states, the calculated t_{2g} quasi-particle spectra for the rutile phase of VO_2 exhibit two spectral features, a coherent peak near E_F and a lower Hubbard band near -1eV , in agreement with experiment. The peak near E_F accounts for the band narrowing and lifetime broadening of the metallic states whereas the Hubbard band is associated with incoherent emission. Since the t_{2g} subbands have comparable single particle distributions their quasi-particle spectra reveal similar correlation features. Moreover, because of the weak orbital polarization in the rutile structure static correlations are negligible. Thus, in the metallic phase the spectral weight transfer between coherent and incoherent contributions to the spectrum is primarily the result of dynamical correlations.

We point out that, in view of the approximate nature of the model underlying the DMFT, quantitative agreement with photoemission data cannot be expected. On the theoretical side, the consideration of purely on-site Coulomb interactions and the neglect of the momentum variation of the self-energy permit only a qualitative analysis of the spectra. In addition, there exists some uncertainty regarding the precise values of the Coulomb and exchange energies. Finally, the DMFT results depend on the temperature used in the QMC calculation. The comparison with results obtained for slightly different values of U , J and T , however, gives us confidence that in the metallic phase the transfer of spectral weight from the coherent peak near E_F to the satellite region near -1eV is qualitatively reliable and consistent with analogous dynamical correlation effects in other $3d^1$ transition metal oxides, such as SrVO_3 .^{23,24,28} As we discuss below, the local DMFT treatment predicts the monoclinic phase to be also metallic. The metal insulator transition in VO_2 is therefore not achieved simply by lowering the temperature in the rutile phase. The lattice transformation from the rutile to monoclinic structure must be taken into account. Therefore, the DMFT results shown in Fig. 3(a) for the rutile structure at $T = 500\text{K}$ can be regarded as representative of correlation induced behavior in the metallic domain.

On the experimental side, as pointed out above, it is important to recall that photoemission data taken at low photon energies represent a superposition of bulk and surface contributions. Since correlation effects are observed to be more enhanced at surfaces,^{22,23,24} the relative intensity of the satellite peak near -1eV in the 21.2eV spectra shown in Fig. 1 is considerably more pronounced than at high photon energies¹⁵ at which primarily bulk-like valence states are detected.

Dynamical effects in the metallic phase may also be evaluated within the GW approach¹⁸ which treats long range Coulomb interactions in the random phase approximation (RPA) and which has proven rather useful to de-

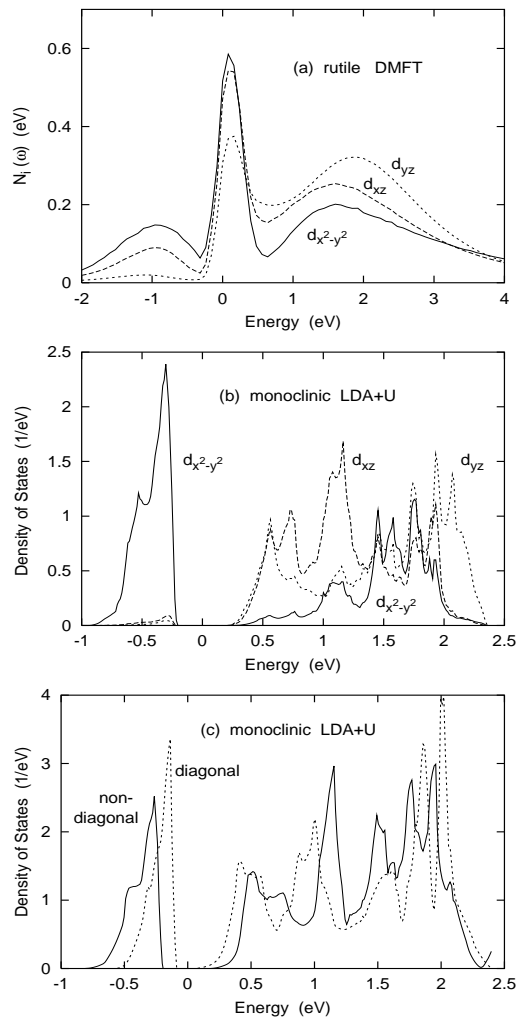


FIG. 3: (a) VO_2 t_{2g} quasi-particle spectra for rutile phase calculated within DMFT; (b) t_{2g} partial density of states for monoclinic phase calculated within LDA+U; (c) monoclinic density of states calculated within non-diagonal (solid curve) and diagonal (dashed curve) versions of the LDA+U; see text. Note the different energy scales.

scribe excitation spectra of weakly correlated systems.²⁹ Because of the neglect of multiple electron-electron and hole-hole scattering processes, this scheme fails when local Coulomb interactions are important.³⁰ Presumably, therefore, for VO_2 the GW method does not reproduce the lower Hubbard band. The satellite in the rutile phase is, of course, also beyond the scope of the static LDA+U approach.³¹ The qualitative agreement between the measured high-temperature spectra and the theoretical results shown in Fig. 2(a) suggests that the DMFT captures the key spectral weight rearrangement induced by dynamical correlations.

B. Insulating Monoclinic Phase

Turning now to the monoclinic phase we first calculated the t_{2g} quasi-particle spectra within the DMFT. Because of the orbital polarization caused by the V-V Peierls distortion, correlation effects in the $d_{x^2-y^2}$ band are now stronger so that the intensity of the lower Hubbard band is enhanced compared to the rutile phase (not shown). While this trend agrees with the photoemission data, the coherent peak near E_F persists. Thus, the single-site DMFT based on a diagonal self-energy does not reproduce the insulating nature of the monoclinic phase.³² This failure is in striking contrast to the results obtained within the LDA+U and *GW* methods.^{10,12}

Let us discuss first the LDA+U approach. In this scheme different orbital occupations give rise to orbital dependent potential terms which shift different t_{2g} bands in opposite directions. Thus, orbital polarization leads to strong *static* correlation effects. Using the same Coulomb parameters as for the rutile phase we find that the local density of states calculated via the LAPW/LDA+U exhibits a gap of about 0.7 eV (see Fig. 3(b)), in agreement with optical data²¹ and previous LDA+U results.¹⁰ The bonding $d_{x^2-y^2}$ bands are now completely filled and the $d_{xz,yz}$ and anti-bonding $d_{x^2-y^2}$ bands are shifted upwards. Thus, the LDA orbital polarization in the monoclinic phase is further increased as a result of static correlations. In turn, this reduction of orbital degeneracy enhances the trend towards insulating behavior.³³

We emphasize that the LDA+U does not provide a complete description of correlation effects in the insulating phase. Essentially, it amounts to a fully self-consistent, non-local treatment of static screening within the dimerized structure. Genuine dynamical effects, such as the spectral weight transfer from the coherent to the incoherent peak as observed in the metallic phase are ignored. Nevertheless, since static correlations appear to be the origin of the excitation gap in VO₂, it is instructive to inquire which features of the LDA+U contribute to the opening of the gap. Of particular interest is the role of the non-diagonal occupation matrix $n_{\alpha\beta}$ which is the key input quantity in the orbital dependent perturbation potential used in the LDA+U. Recent work by Pavarini *et al.*²⁸ on 3d¹ perovskite materials exhibiting non-diagonal t_{2g} orbital coupling caused by octahedral distortions suggests that this mechanism tends to suppress orbital fluctuations and to enhance insulating behavior. Fig. 3(c) compares the VO₂ LDA+U density of states with results of an approximate LDA+U treatment in which at each iteration only the diagonal elements $n_{\alpha\alpha}$ are retained. The size of the gap is seen to be only slightly reduced. In the case of VO₂, therefore, non-diagonal coupling among t_{2g} orbitals is evidently not the main reason for the existence of the gap.

To understand the gap formation obtained within the LDA+U, it is useful to formally express the t_{2g} self-energy matrix as $\Sigma(\omega, k) = \Sigma^{\text{HF}}(k) + \Delta\Sigma(\omega, k)$, where $\Sigma^{\text{HF}}(k) = H^{\text{LDA+U}}(k) - H^{\text{LDA}}(k)$ is real and accounts

for spectral changes associated with the LDA+U.³⁴ $\Delta\Sigma(\omega, k)$ is complex and describes purely dynamical effects. The important point is that the LDA+U includes the full momentum variation of $\Sigma^{\text{HF}}(k)$ within the true lattice geometry. Thus, in a site representation, static screening processes generate finite inter-site elements $\Sigma_{i\neq j}^{\text{HF}}$ (each element is a matrix in orbital space) even if the bare LDA+U perturbation potential is site-diagonal. Thus, $\Sigma_{ij}^{\text{HF}}(k)$ is more accurate than the static limit of the single-site DMFT which neglects the k dependence and assumes the impurity environment to be isotropic, i.e., $\Sigma_{ij}^{\text{DMFT}}(\omega) \sim \delta_{ij}$. The results shown in Fig. 3(b,c) suggest that the proper evaluation of $\Sigma^{\text{HF}}(k)$ within the Brillouin Zone of the dimerized structure is the crucial ingredient to an adequate description of the insulating behavior in VO₂. The LDA+U amounts to a self-consistent treatment of $\Sigma^{\text{HF}}(k)$ since the solution of the Schrödinger equation imposes no restrictions on how the wave functions adjust to the LDA+U potential.

In order to go beyond static screening and include dynamical correlations in the monoclinic phase a cluster extension of the DMFT is most likely required. Such an extension is beyond the scope of the present work. A cluster DMFT would include the crucial inter-site elements $\Sigma_{i\neq j}^{\text{DMFT}}(\omega)$ which arise naturally in a cluster representation of the lattice and of the impurity Green's functions $G(\omega)$ and $G_0(\omega)$, even for a purely on-site Coulomb interaction. Preliminary results for VO₂ within a cluster DMFT³⁵ show that dynamical screening processes beyond the static correlations included in the LDA+U cause a broadening of the LDA+U density distribution and a shift of the main spectral peak towards the Hubbard bands. Possibly, a multi-site extension of the DMFT might also identify the true origin of the metal insulator transition in VO₂, i.e., whether it is primarily caused by the lattice reconstruction or by Coulomb correlations, or whether these mechanisms mutually enhance each other. All one can say at present is that, given the orbital polarization induced by the lattice transition, Coulomb correlations have a pronounced effect on the quasi-particle spectra.

As noted above, the *GW* approach applied to the monoclinic phase of VO₂ also yields an excitation gap of the correct magnitude.¹² These calculations utilize a model self-energy³⁶ consisting of an approximate short-range contribution given by the local exchange correlation potential, and a correction due to incomplete screening of the Coulomb interaction. Essentially, in this simplified *GW* scheme the self-energy correction consists of a “scissor” operator and additional, non-rigid shifts of energy eigenvalues.³⁶ Presumably, the reason why this model self-energy yields a gap is that $\Sigma(q, \omega)$ is non-local and non-diagonal in site space, i.e., it includes the important static correlations in the dimerized structure in a similar fashion as the LDA+U. The approximate nature of the *GW* method, in particular, the neglect of electron-electron and hole-hole ladder type interactions, affects mainly the remaining dynamical corrections caused by

the strong local Coulomb energy. An adequate treatment of these corrections would require going beyond the RPA and should lead to a more realistic description of the position and width of the Hubbard bands.

An interesting additional feature observed by Okazaki *et al.*¹⁴ is the temperature dependence of the photoemission spectra below the metal insulator transition. Essentially, towards lower T the excitation gap becomes more clearly defined and the main peak near -1 eV gets slightly sharper. These changes, however, are very small on the scale of the main discrepancy still existing between the LDA+U or GW results and the experimental data. At present it is not clear whether cluster DMFT calculations in the monoclinic phase as a function of temperature will be able to explain the observed trend or whether an explicit treatment of electron-phonon coupling is required.

III. SUMMARY

The metal insulator transition in VO_2 appears to be remarkably complex and its origins are not yet fully understood. In the present work we focussed on the important role of two aspects, local Coulomb correlations

and orbital polarization, in the low and high temperature photoemission spectra of VO_2 . Whereas the metallic phase exhibits weak static and strong dynamical correlations, the monoclinic phase is dominated by static Coulomb correlations. Accordingly, the rutile spectra reveal a double-peak structure where the feature close to E_F is identified with metallic V $3d$ states and the peak near -1 eV with the lower Hubbard band. Since the t_{2g} states in the metallic phase are roughly equally occupied orbital polarization is negligible. The fundamental difference in the monoclinic phase is the large orbital polarization induced by the symmetry breaking due to V-V dimerization. The preferential occupation of the $d_{x^2-y^2}$ bonding states implies strong static correlations which are the main origin of the excitation gap. It would be of great interest to study the additional dynamical correlation effects in this phase within an extension of the single-site DMFT approach.

A. L. likes to thank K. Okazaki, A. Fujimori, and L.H. Tjeng for sharing their photoemission data prior to publication. He also thanks F. Aryasetiawan, A. Bringer, K. Held, G. Kotliar, A. I. Lichtenstein, A. Poteryaev, and D. Vollhardt for fruitful discussions.

email: a.liebsch@fz-juelich.de; ishida@chs.nihon-u.ac.jp; g.bihlmayer@fz-juelich.de

-
- ¹ F. J. Morin, Phys. Rev. Lett. **3**, 34 (1959).
² J. P. Pouget, H. Launois, T. M. Rice, P. Dernier, A. Gosard, G. Villeneuve, and P. Hagenmuller, Phys. Rev. B **10**, 1801 (1977); J. P. Pouget, H. Launois, J. P. D'Haenens, P. Merender, and T. M. Rice, Phys. Rev. Lett. **35**, 873 (1975).
³ A. Zylbersztejn and N. F. Mott, Phys. Rev. B **11**, 4384 (1975);
⁴ N. F. Mott, *Metal Insulator Transitions* (Taylor and Francis, London, 1990).
⁵ T. M. Rice, H. Launois, and J. P. Pouget, Phys. Rev. Lett. **73**, 3042 (1994).
⁶ J. B. Goodenough, Phys. Rev. **117**, 1442 (1960).
⁷ E. Caruthers and L. Kleinman, Phys. Rev. B **7**, 3760 (1973).
⁸ R. M. Wentzcovitch, W. W. Schulz, and P. B. Allen, Phys. Rev. Lett. **72**, 3389 (1994); *ibid.* **73**, 3043 (1994).
⁹ V. Eyert, Ann. Phys. **11**, 9 (2002).
¹⁰ X. Huang, W. Yang, and U. Eckern, cond-mat/9808137.
¹¹ M. A. Korotin, N. A. Skorikov, and V. I. Anisimov, cond-mat/0301347.
¹² A. Continenza, S. Massida, and M. Posternak, Phys. Rev. B **60**, 15699 (1999).
¹³ M. S. Laad, L. Craco and E. Müller-Hartmann, cond-mat/0305081.
¹⁴ K. Okazaki, H. Wadati, A. Fujimori, M. Onoda, Y. Muraoka and Z. Hiroi, Phys. Rev. B. **69**, 165104 (2004).
¹⁵ L. H. Tjeng *et al.*, to be published.
¹⁶ For a review, see: A. Georges, G. Kotliar, W. Krauth and M. J. Rozenberg, Rev. Mod. Phys. **68**, 13 (1996).
¹⁷ V. I. Anisimov, J. Zaanen, and O. K. Andersen, Phys. Rev. B **44**, 943 (1991); A. I. Lichtenstein, V. I. Anisimov, and J. Zaanen, Phys. Rev. B **52**, R5467 (1995).
¹⁸ L. Hedin, Phys. Rev. A **139**, 796 (1965).
¹⁹ Y. Muraoka, Y. Ueda, and Z. Hiroi, J. Phys. Chem. Solids **63**, 965 (2002).
²⁰ G. A. Sawatzky and D. Post, Phys. Rev. B **20**, 1546 (1979); V. M. Bermudez *et al.*, *ibid.* **45**, 9266 (1992); E. Goering *et al.*, *ibid.* **55**, 4225 (1997).
²¹ S. Shin, S. Suga, M. Taniguchi, M. Fujisawa, H. Kanazaki, A. Fujimori, H. Daimon, Y. Ueda, K. Kosuge, and S. Kachi, Phys. Rev. B **41**, 4993 (1990).
²² K. Maiti, D. D. Sarma, M. J. Rozenberg, I. H. Inoue, H. Makino, O. Goto, M. Pedio, and R. Cimino, Europhys. Lett. **55**, 246 (2001).
²³ A. Sekiyama, H. Fujiwara, S. Imada, S. Suga, H. Eisaki, S.I. Uchida, K. Takegahara, H. Harima, Y. Saitoh, I. A. Nekrasov, G. Keller, D. E. Kondakov, A. V. Kozhevnikov, Th. Pruschke, K. Held, D. Vollhardt, and A. I. Anisimov, Phys. Rev. Lett., to be published.
²⁴ A. Liebsch, Phys. Rev. Lett. **90**, 96401 (2003).
²⁵ J. P. Perdew and Y. Wang, Phys. Rev. B **45**, 13244 (1992).
²⁶ W. E. Pickett, S. C. Erwin, and E. C. Ethridge, Phys. Rev. B **58**, 1201 (1998).
²⁷ M. Jarrell and J. E. Gubernatis, Phys. Rep. **269**, 133 (1996).
²⁸ E. Pavarini, S. Biermann, A. Poteryaev, A. I. Lichtenstein, A. Georges, and O. K. Andersen, Phys. Rev. Lett. **92**, 176403 (2004).
²⁹ W. G. Aulbur, L. Jönsson and J. W. Wilkins, *Quasiparticle Calculations in Solids*, Solid State Physics, eds. H. Ehrenreich and F. Spaepen (Academic, San Diego, 2000), Vol. 54, p. 1.
³⁰ F. Aryasetiawan and O. Gunnarsson, Rep. Progr. Phys. **61**, 237 (1997).

- ³¹ As shown by Huang *et al.*,¹⁰ in the rutile phase the LDA+U gives a gap only at unrealistically large values of U . The gap in the insulating phase therefore requires pronounced orbital polarization.
- ³² This finding agrees with: K. Held *et al.*, private communication.
- ³³ O. Gunnarsson *et al.*, Phys. Rev. B **54**, R11026 (1996); E. Koch *et al.*, Phys. Rev. B **60**, 15714 (1999); S. Florens *et al.*, Phys. Rev. B **66**, 205102 (2002).
- ³⁴ I. Yang, S. Y. Savrasov, and G. Kotliar, cond-mat/0209073.
- ³⁵ A. Poteryaev and A. I. Lichtenstein, private communication.
- ³⁶ F. Gygi and A. Baldereschi, Phys. Rev. Lett. **62**,2160 (1989).